Adsorption (2010) 16: 173–181
DOI 10.1007/s10450-010-9220-7

Adsorption kinetic, thermodynamic and desorption studies of phosphate onto hydrous niobium oxide prepared by reverse microemulsion method

Liana Alvares Rodrigues · Maria Lúcia Caetano Pinto da Silva

Received: 23 October 2008 / Accepted: 24 May 2010 / Published online: 9 June 2010

Abstract A type of $Nb_2O_5{\cdot}3H_2O$ was synthesized and its phosphate removal potential was investigated in this study. The kinetic study, adsorption isotherm, pH effect, thermodynamic study and desorption were examined in batch experiments. The kinetic process was described by a pseudo-second-order rate model very well. The phosphate adsorption tended to increase with a decrease of pH. The adsorption data fitted well to the Langmuir model with which the maximum P adsorption capacity was estimated to be 18.36 mg-P g^{-1}. The peak appearing at 1050 cm^{-1} in IR spectra after adsorption was attributed to the bending vibration of adsorbed phosphate. The positive values of both ΔH° and ΔS° suggest an endothermic reaction and increase in randomness at the solid-liquid interface during the adsorption. ΔG° values obtained were negative indicating a spontaneous adsorption process. A phosphate desorbability of approximately 68% was observed with water at pH 12, which indicated a relatively strong bonding between the adsorbed phosphate and the sorptive sites on the surface of the adsorbent. The immobilization of phosphate probably occurs by the mechanisms of ion exchange and physicochemical attraction. Due to its high adsorption capacity, this type of hydrous niobium oxide has the potential for application to control phosphorus pollution.

Keywords Adsorption · Hydrous niobium oxide · Phosphate · Desorption

L.A. Rodrigues · M.L.C.P. da Silva (✉)
Escola de Engenharia de Lorena, Universidade de São Paulo, CP. 116, 12600-000 Lorena, SP, Brazil
e-mail: mlcaetano@dequi.eel.usp.br

1 Introduction

Phosphates are used in many consumer products and industrial processes that involve particles of a colloidal nature. Examples of such applications are as diverse as fertilizes, detergents, pigment formulation, water treatment and mineral processing (Namasivayam and Sangeetha 2004).

Though it is essential nutrient for growth of microorganisms in aquatic environments, concentration in excess of desired limit causes eutrophication of lakes, lagoons, rivers and sea thereby posing serious concern. The increased nutrient concentrations can result in a bloom in phytoplankton and degradation of water quality due to alterations in nutrient ratios (Das et al. 2006; Ye et al. 2006). Consequently, the removal of phosphates from surface water is absolutely necessary to avoid any kind of problems. Wastes containing phosphate must meet the maximum discharge limits (Karageorgiou et al. 2007). In Brazil, these limits are determined by National Environment Council (*Conselho Nacional do Meio Ambiente*, CONAMA). The maximum P concentration allowed is 0.02 mg L^{-1} (Rodgher et al. 2005).

In wastewater treatment technology, various techniques have been used for phosphate removal. Phosphorus removal techniques fall into three main categories: physical, chemical and biological. Chemical treatments are more effective for phosphate removal, but there are problems of sludge handling, its disposal and neutralization of the effluent. Physical methods have proved to be either too expensive, as in the case of electrodialysis and reverse osmosis, or inefficient, removing only 10% of the total phosphorus. Enhanced biological treatment can remove up to 97% of total phosphorus, but this process can be highly variable due operational difficulties (Oguz 2005; Spinelli et al. 2005; Rodrigues and Silva 2008). Adsorption is one of the techniques that would be comparatively more useful and economical for this aim (Karaca et al. 2004; Wang et al. 2007;

Krishnan and Haridas 2008). The application of low-cost and easily available materials has been widely used for phosphate removal. These include layered double hydroxides (Chitrakar et al. 2005), individual and mixed hydrous oxides (Borggaard et al. 2005; Manna and Ghosh 2007; Chubar et al. 2005; Harvey and Rhue 2008), metal oxides (Liu et al. 2008), hybrid materials (Mulinari et al. 2007; Blaney et al. 2007), red mud (Huang et al. 2008), goethite (Luengo et al. 2006; Zhong et al. 2007; Nowack and Stone 2006) and steel slag (Xiong et al. 2008). Among these materials, hydrous metal oxides have a relatively strong affinity to phosphate (Antelo et al. 2007).

Hydrous niobium oxide has remarkable selectivity to phosphate ions, and also high resistance against attacks by acids, alkalis, oxidants and reductants, which mean that it has great potential to immobilize phosphate from water (Antelo et al. 2005; Tagliaferro et al. 2005).

The present work describes the kinetics, isotherm and thermodynamics of phosphate adsorption from aqueous solutions onto hydrous niobium oxide ($Nb_2O_5{\cdot}nH_2O$) prepared by reverse microemulsion method.

2 Experimental

2.1 Synthesis of hydrous niobium oxide by reverse microemulsion method

The microemulsion system water/heptane/butanol/cetyltrimethylammonium bromide (CTAB) was chosen as reaction medium for carrying out the precipitation of hydrous niobium oxide ($Nb_2O_5{\cdot}nH_2O$). Then the CTAB used as surfactant (S) and the butanol used as cosurfactant (C) were mixed with weight ratio 8:1 by magnetically stirring. Two microemulsions were prepared as follows: ME1—31.28% (%w) heptane, 58.09% butanol/CTAB (C/S) and 10.63% $NbOF_5^{-2}$/water (1:2, v/v); ME2—31.28% heptane, 58.09% butanol/CTAB (C/S) and 10.63% NH_4OH. All experimental processes were under magnetic stirring. ME1 was added dropwise to the ME2 under stirring. Then the two solutions were mixed and magnetically stirred for 3 min at room temperature. The precipitates were collected by centrifugation, followed by filtration and repeatedly washed using water and ethanol. The $Nb_2O_5{\cdot}nH_2O$ was dried in an oven at 50 °C until a constant weight was achieved. $NbOF_5^{-2}$ was prepared by dissolution of metallic niobium in HNO_3 (65%)/HF (40%) mixtures (1:3 molar).

2.2 Characterization

Thermogravimetry measurement (TG/DTG) was carried out with a Shimadzu TGA-50 thermal analyzer from 25 to 800 °C at a heating rate of 20 °C min^{-1} in N_2 atmosphere.

BET surface area measurement was carried out using Quantachrome NOVA 1200. The samples were degassed at 50 °C for 16 h in vacuum prior to analysis. The nitrogen adsorption was carried out at 77 K.

The IR spectra of hydrous niobium oxide were taken before and after the adsorption tests on a Perkin Elmer Spectrun One spectrophometer as KBr pellets in the range of 4000–500 cm^{-1}.

2.3 Adsorption studies

All adsorption studies were carried out in polyethylene flasks of 100 mL by subjecting a given dose of hydrous niobium oxide to a period of shaking with 50 mL of phosphate solution on a thermostated orbital shaker. The pH of phosphate solution was adjusted using dilute HCl and NaOH solutions by using pH meter. The supernatant solution was separated from the adsorbent by filtration. Phosphate concentration in the supernatant was estimated spectrophotometrically by the molybdenum blue method, monitoring the absorbance at 880 nm on UV-vis spectrophotometer (Radojevic and Bashkin 1999). The range of detected phosphate concentration in this method is 1.2 mg L^{-1}. The samples containing more phosphate than the highest concentration of detected (1.2 mg L^{-1}) were diluted, and the dilution was corrected when calculating the result. The adsorption studies with phosphate synthetic solutions were performed using the following conditions:

Kinetic study Hydrous niobium oxide dose 2 g L^{-1}; initial phosphate concentrations 10, 30 and 50 mg L^{-1}; pH 2; shaking time 0–7 h; $T = 25$ °C.

Effect of pH Hydrous niobium oxide dose 2 g L^{-1}; initial phosphate concentration 50 mg L^{-1}; pH 2–9; predetermined shaking time value; $T = 25$ °C.

Adsorption isotherms Hydrous niobium oxide dose 2 g L^{-1}; initial phosphate concentrations 10–50 mg L^{-1}; predetermined pH; predetermined shaking time value; $T = 25$ °C.

Thermodynamic study Hydrous niobium oxide dose 2 g L^{-1}; initial phosphate concentrations 50 mg L^{-1}; predetermined pH; predetermined shaking time value; temperature range 25–65 °C.

Desorption The adsorbent that was used for the adsorption of 50 mg L^{-1} of phosphate solution was separated from the solution by filtration and washed gently with water to remove any unadsorbed phosphate. Then the spent adsorbent was mixed with 50 mL of distilled water at pH 5 and 12, adjusted using dilute HCl and NaOH solutions, and agitated at time intervals not longer than the equilibrium time. The desorbed phosphate was estimated as before.

3 Results and discussion

3.1 Thermal analysis and BET measurements

The TG curve (Fig. 1) revealed that the first weight loss (about 18%) was caused by the desorption of physically adsorbed water (Tagliaferro et al. 2005). The degree of hydration in the hydrous niobium oxide was determined from the weight loss between 25 and 800 °C. TG data indicated that the chemical formula of the hydrous niobium oxide prepared was $Nb_2O_5{\cdot}3H_2O$.

The BET specific surface area was 60 $m^2\,g^{-1}$ much smaller than the 166 and 89 $m^2\,g^{-1}$ observed on the AlOOH and α-Al_2O_3 reported literature data for phosphate removal (Xiaofang et al. 2007), and 232 $m^2\,g^{-1}$ reported for phosphate removal onto ZrO_2 (Liu et al. 2008).

3.2 Kinetic study

The kinetic curves obtained for the adsorption of phosphate from aqueous solutions onto hydrous niobium oxide are shown in Fig. 2. These curves clearly show that the time required to reach equilibrium depends on the initial phosphate concentration. For the highest value (50 mg L^{-1}) adsorption increased sharply at short contact times and slowed gradually as equilibrium was approached; 5 h of interaction were needed to attain values above 80% of the phosphate amount adsorbed at equilibrium. For the middle and lowest concentration (30 and 10 mg L^{-1}), the equilibrium was attained after 60 and 30 min of interaction, respectively. About 75% (30 mg L^{-1}) and 99% (10 mg L^{-1}) of the phosphate were adsorbed after equilibrium.

Up to now, several kinetic models such as the pseudo first- and second-order equations and intraparticle diffusion equation are used to examine the controlling mechanism of adsorption process (Hameed et al. 2007; Chen et al. 2007). The linear pseudo first-order equation is given as follows:

$$\log(q_e - q_t) = \log q_e - \frac{k_1 t}{2{,}303} \quad (1)$$

where q_t and q_e are the amounts of phosphate adsorbed at time and at equilibrium (mg g^{-1}), respectively, and k_1 is the rate constant of pseudo first-order adsorption process (h^{-1}). The slopes and intercepts of plots of $\log(q_e - q_t)$ versus t (Fig. 3) were used to determine the first-order rate constant k_1 and equilibrium adsorption density q_e. A comparison of the results with the correlation coefficients is shown in Table 1. The correlation coefficients for the first-order kinetic model obtained at all the studied concentra-

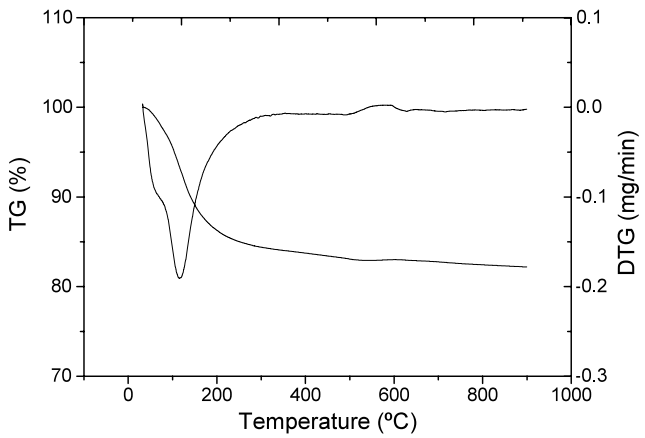

Fig. 1 TG/DTG curves of hydrous niobium oxide synthesized

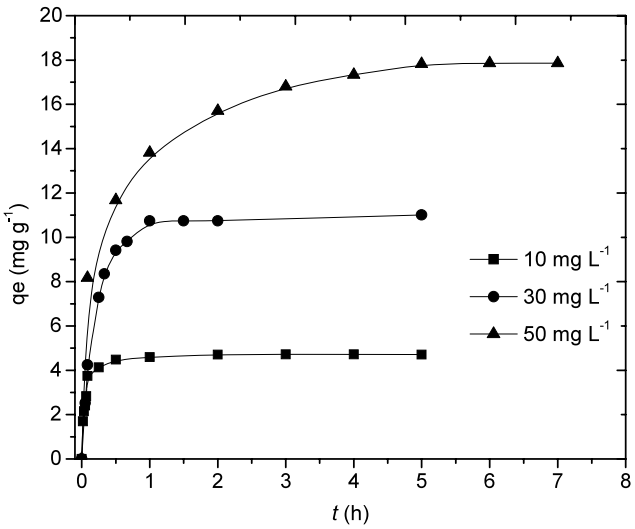

Fig. 2 The variation of adsorption capacity with adsorption time at various initial phosphate concentrations (T = 25 °C; adsorbent dose = 2 g L^{-1}; pH = 2)

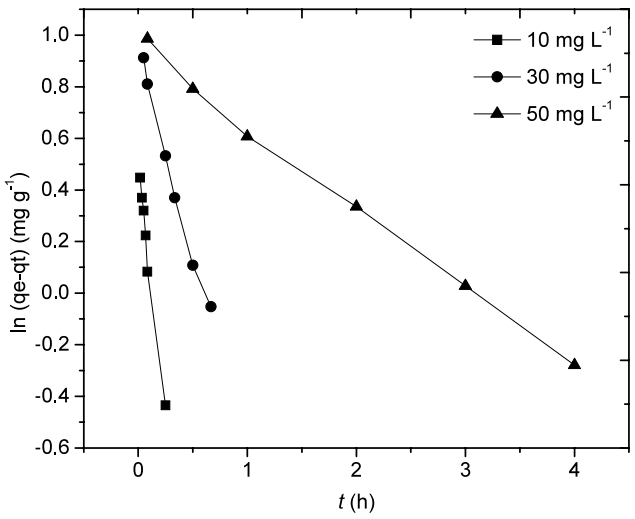

Fig. 3 Pseudo-first-order kinetics for adsorption of phosphate onto $Nb_2O_5{\cdot}3H_2O$

Table 1 Kinetic parameters for phosphate adsorption onto $Nb_2O_5{\cdot}3H_2O$

C_0 (mg L^{-1})	First-order-model			Second-order-model			Intraparticle diffusion	
	k_1 (h^{-1})	q_1 (mg g^{-1})	R^2	k_2 (g mg^{-1} h^{-1})	q_2 (mg g^{-1})	R^2	k_{in} (mg g^{-1} $h^{-1/2}$)	R^2
50	0.72	9.21	0.99	0.24	18.10	1.00	5.94	0.95
30	3.64	8.77	0.98	0.43	12.68	1.00	12.85	0.97
10	8.62	4.72	0.98	4.96	4.77	0.99	1.22	0.87

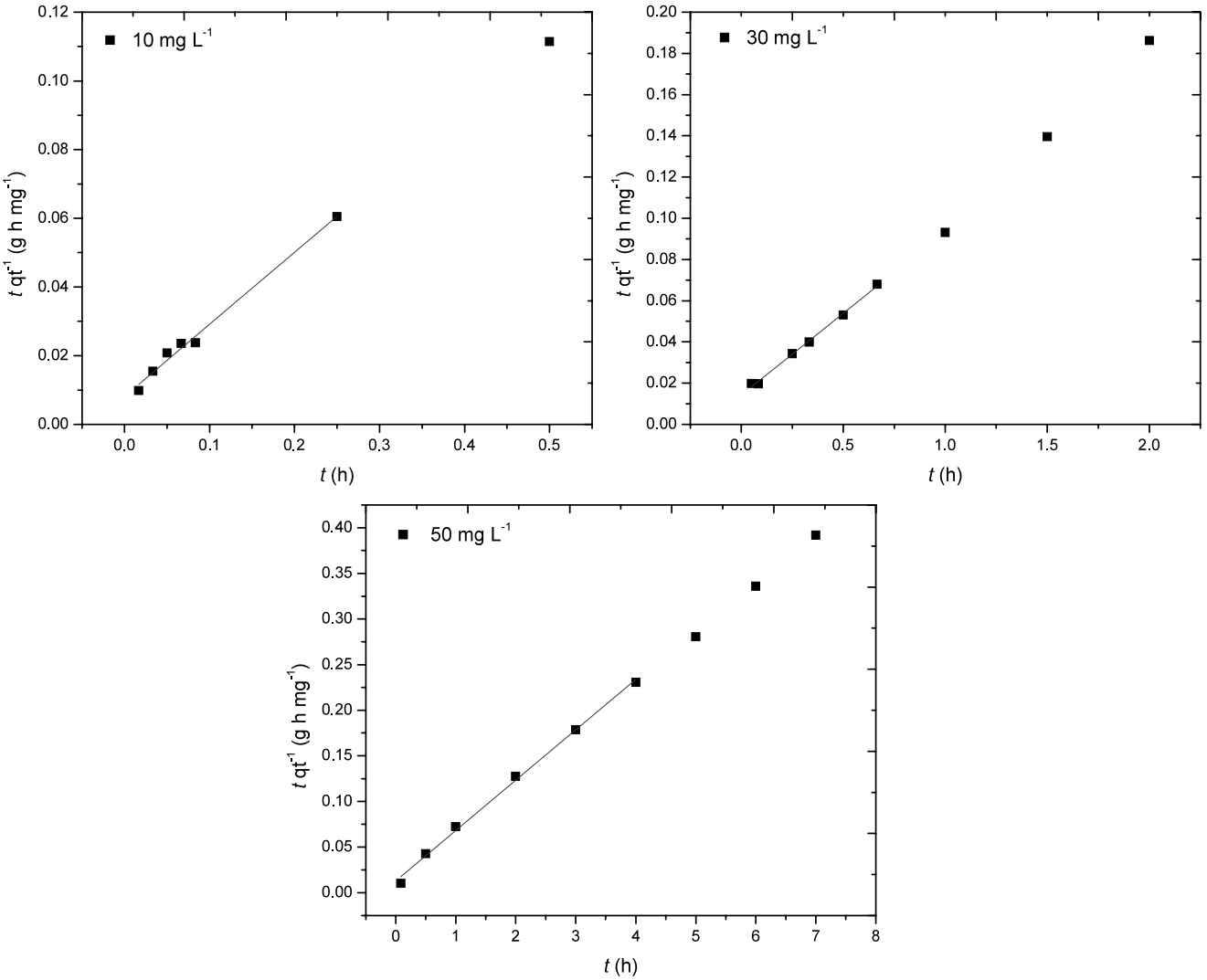

Fig. 4 Pseudo-second-order kinetics for adsorption of phosphate onto $Nb_2O_5{\cdot}3H_2O$

tions were lower than obtained for the second-order kinetic model. It was also observed in the present work that q_e values computed from the Lagergren plots deviated considerably from the experimental q_e values. This indicates that pseudo first-order equation might not be sufficient to describe the mechanism of phosphate-hydrous niobium oxide interactions. The linear pseudo second-order equation is given as follows:

$$\frac{t}{q_t} = \frac{1}{k_2 q_e^2} + \frac{t}{q_t} \tag{2}$$

where k_2 is the pseudo second-order rate constant (g mg^{-1} h^{-1}). The slopes of the plots tq_t^{-1} versus t give the value of q_e, and from the intercept k_2 can be calculated. The plot of tq_t^{-1} versus t (Fig. 4) yields very good straight lines for different initial phosphate concentrations. Table 1 lists the computed results obtained from

the second-order equation. The correlation coefficients for the second-order kinetic equation were higher for all concentrations. The calculated q_e values also agree very well with the experimental data. These indicate that the adsorption system studied belongs to the second order kinetic model. The pseudo second-order rate constant decreased from 4.96 to 0.24 $g\,mg^{-1}\,h^{-1}$ when the phosphate initial concentration increased from 10 to 50 $mg\,L^{-1}$. Similar kinetic results have also been reported by Özacar (2006).

The variation in the amount of adsorption with time at different initial phosphate ion concentrations can be used to evaluate the role of diffusion in the adsorption process. The intraparticle diffusion rate constant (k_{dif}) is given by the equation:

$$q_t = k_{dif} t^{0,5} \tag{3}$$

where k_{dif} is intraparticular diffusion rate constant ($mg\,g^{-1}\,h^{-1/2}$). Such plots may present a multilinearity, indicating that two or more steps take place. The first, sharper portion is attributed to the diffusion of adsorbate through the solution to the external surface of adsorbent or the boundary layer diffusion of solute molecules or ions. The second portion describes the gradual adsorption stage, where intraparticle diffusion is rate limiting. The third portion is attributed to the final equilibrium stage where intraparticle diffusion starts to slow down due to extremely low adsorbate concentrations in the solution (Lorenc-Grabowska and Gryglewicz 2005). Figure 5 shows a plot of the linearized form of the intraparticle diffusion model at all concentrations studied. It can be seen that the plots are not linear over the whole time range, implying that more than one process affects the phosphate adsorption. The rate parameters, k_{dif}, together with the correlation coefficients are also listed in Table 1.

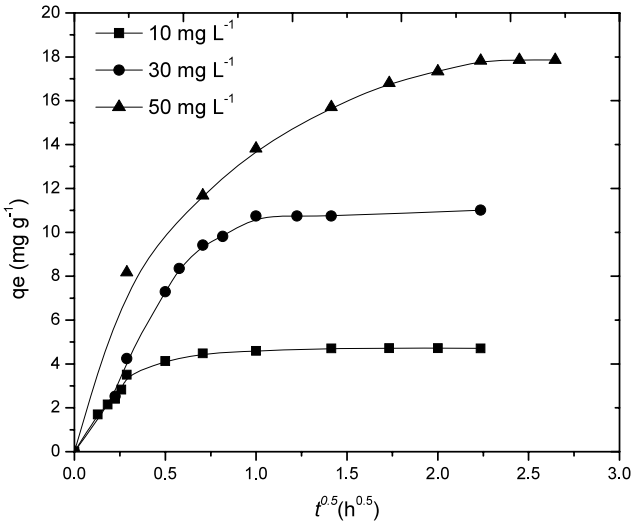

Fig. 5 Intraparticle diffusion kinetics for adsorption of phosphate onto $Nb_2O_5{\cdot}3H_2O$

The pseudo second-order kinetic model provides the best correlation for all of the adsorption process.

3.3 Effect of pH

The pH of the aqueous solution is an important variable, which influences the adsorption of both anions and cations at the solid–liquid interface. The anion exchange capacity is strongly governed by the pH of the solution and by the surface chemistry of the solids. The effect of pH on phosphate adsorption onto the hydrous niobium oxide is shown in Fig. 6. It is found that while the adsorbed amount of phosphate increased from 2.2 to 17.2 mg-P g^{-1} with a decrease in pH from 9 to 2. The results showed that the phosphate adsorption is strongly pH dependent. The value of zero point charge (PZC) of hydrous niobium oxide reported in the literature was close to 3.5 (Inoue et al. 1988). The pH dependency is both related to the amphoteric properties of the hydrous niobium oxide surface and to the polyprotic nature of phosphate. Phosphate can exist in different ionic species such as monovalent $H_2PO_4^-$, divalent HPO_4^{2-}, and trivalent PO_4^{3-} ions, depending on the pH of the solution (pK1 = 2.15, pK2 = 7.20, pK3 = 12.33) (Chitrakar et al. 2006). The pH dependence of the uptake is likely attributable to the fact that a lower pH causes the hydrous niobium oxide surface to carry a more positive charge, and thus would more significantly attract the negatively charged monovalent $H_2PO_4^-$ ions in solution, which indicated that the physicochemical adsorption due to Coulombic attraction was the predominant process of P removal. In the lower pH range, Coulombic attraction can readily occur in conjunction with specific chemical adsorption due to an exchange reaction (Liu et al. 2008). When pH of the solution increases, the surface becomes negatively charged and the adsorption capacity for phosphate decreases. Because negatively charged

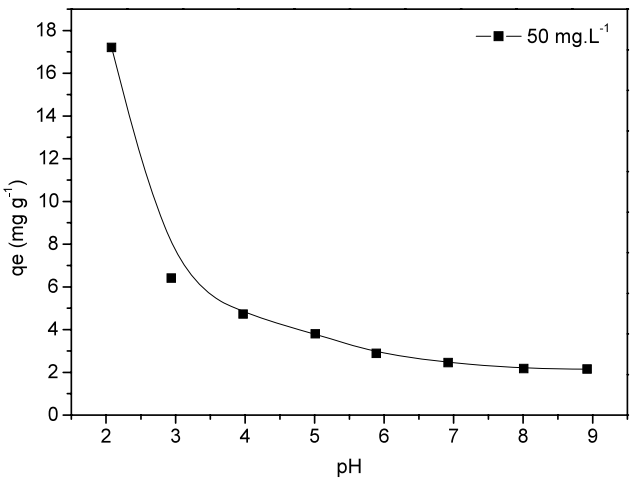

Fig. 6 Effect of solution pH on the adsorption of phosphate onto $Nb_2O_5{\cdot}3H_2O$ (C_0 = 50 $mg\,L^{-1}$; T = 25 °C; adsorbent dose = 2 $g\,L^{-1}$; t = 5 h)

surface sites on the adsorbent unfavors of phosphate due to the electrostatic repulsion. Therefore, maximum phosphate adsorption occurred at pH 2. The similar pH dependence of the anion adsorption is generally observed in trivalent and tetravalent metal hydroxides (Chitrakar et al. 2006).

3.4 Adsorption isotherms

Adsorption isotherms are mathematical models that describe the distribution of the adsorbate species among liquid and adsorbent, based on a set of assumptions that are mainly related to the heterogeneity/homogeneity of adsorbents, the type of coverage, and possibility of interaction between the adsorbate species. The Langmuir model assumes that there is no interaction between the adsorbate molecules and the adsorption is localized in a monolayer (Sodré et al. 2001; Gomri et al. 2006; Limousin et al. 2007). The Freundlich isotherm model is an empirical relationship describing the adsorption of solutes from a liquid to a solid surface, and assumes that different sites with several adsorption energies are involved (Deliyanni et al. 2007). The Freundlich adsorption model is expressed by

$$q_e = K C_e^{1/n} \tag{4}$$

where K_F and $1/n$ are the Freundlich constants.

The Langmuir adsorption model is expressed by

$$q_e = Q_0 b C_e/(1 + bC_e) \tag{5}$$

where Q_0 (mg-P g^{-1}) is the maximum adsorption capacity and b is the binding constant which is relate to the heat of adsorption.

The result of the phosphate adsorption isotherm experiments are shown in Fig. 7. The phosphate adsorption capacity increased with the phosphate equilibrium concentration increasing from 0 to 18 mg-P L^{-1}. Two typical isotherms (Freundlich and Langmuir) were used for fitting the experimental data. The Freundlich and Langmuir constants are presented in Table 2. From Table 2, higher correlation coefficients indicate that the Langmuir model fits the adsorption data better than the Freundlich model. The maximum uptake of phosphate on hydrous niobium oxide was 18.36 mg-P g^{-1} smaller than the 30 mg-P g^{-1} observed on the ZrO_2 reported literature data (Liu et al. 2008), and similar than 14 and 9 mg-P g^{-1} reported for phosphate removal onto AlOOH and α-Al_2O_3 (Xiaofang et al. 2007). Phosphate removal onto $Nb_2O_5{\cdot}3H_2O$ is low as compared to ZrO_2 due to smaller specific surface area and affinity of the anions for the exchange sites.

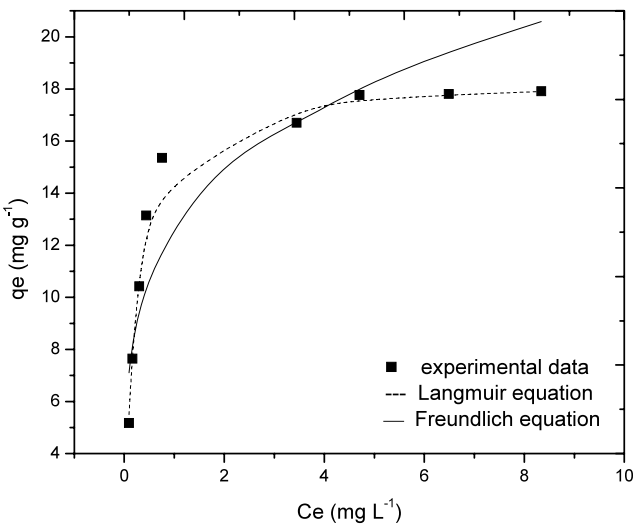

Fig. 7 Phosphate adsorption isotherm (pH = 2; T = 25 °C; adsorbent dose = 2 g L^{-1}; t = 5 h)

3.5 IR

In the IR spectrum of hydrous niobium oxide before adsorption (Fig. 8), a strong and broad band in the 3500–3300 cm^{-1} region (O–H stretching vibration) and a band at 1625 cm^{-1} (O–H bending vibration) indicated the presence of coordinated water molecules, with the peak at 1380 cm^{-1} (O–H bending vibration) indicating the presence of surface hydroxyl on the metal oxide surface. It could be seen that after adsorption, the peak at 1380 cm^{-1} weakened dramatically. The decreasing tendency of this peak indicated that most of the surface hydroxyl groups were replaced by adsorbed phosphate. The peak appearing at 1050 cm^{-1} was

Table 2 Langmuir, Freundlich isotherm constants for adsorption of phosphate onto $Nb_2O_5{\cdot}3H_2O$

Langmuir isotherm model			Freundlich isotherm model		
Q_0 (mg-P g^{-1})	b (L mg^{-1})	R^2	K_F	$1/n$	R^2
18.36	4.71	0.99	8.56	0.24	0.91

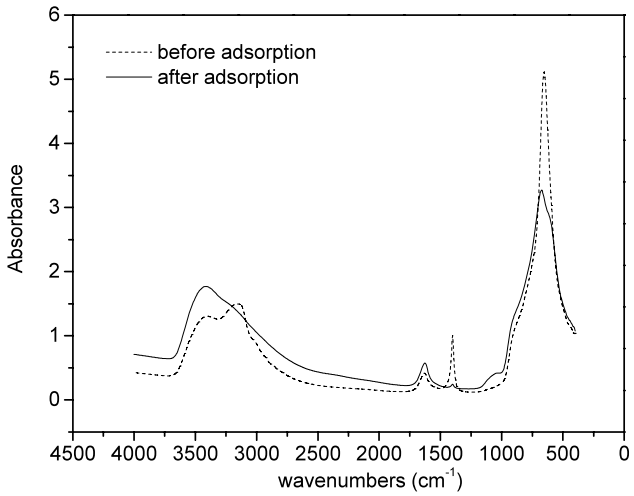

Fig. 8 The IR spectra of $Nb_2O_5{\cdot}3H_2O$ before and after adsorption

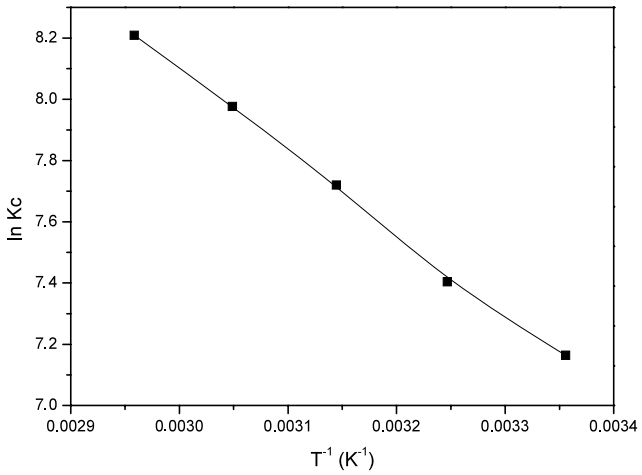

Fig. 9 Plot of $\ln K_c$ vs. T^{-1} for phosphate adsorption onto $Nb_2O_5{\cdot}3H_2O$ (pH = 2; $C_0 = 50\ mg\,L^{-1}$; adsorbent dose = $2\ g\,L^{-1}$; $t = 5$ h)

attributed to the bending vibration of adsorbed phosphate (Liu et al. 2008).

3.6 Thermodynamic study

The thermodynamic parameters such as change in standard free energy (ΔG°), enthalpy (ΔH°) and entropy (ΔS°) were determined by using the following equations:

$$\ln K_c = \frac{\Delta S^\circ}{R} - \frac{\Delta H^\circ}{RT} \tag{6}$$

$$\Delta G^\circ = \Delta H^\circ - T\Delta S^\circ \tag{7}$$

where R (8.314 J/mol K) is the gas constant, T (K) the absolute temperature and K_c (mL/g) is the standard thermodynamic equilibrium constant defined by q_e/C_e. By plotting a graph of $\ln kc$ versus T^{-1} (Fig. 9) the values ΔH° and ΔS° can be estimated from the slopes and intercepts (Hameed et al. 2007). The adsorption of phosphate increases with the increase of temperature (Fig. 9) is positive. Table 3 shows the negative values of ΔG° and positive ΔH° obtained indicated that the phosphate adsorption process is a spontaneous and an endothermic (Unuabonah et al. 2007). The ΔH° value is found to be less than 40 kJ mol^{-1} which indicates the adsorption of phosphate onto hydrous niobium oxide is physisorption (Du et al. 2008; Ren et al. 2008). The decrease in ΔG° with the increase of temperature indicated more efficient adsorption at higher temperature. The positive value of ΔS° suggests increased randomness at the solid/solution interface occur in the internal structure of the phosphate adsorption onto hydrous niobium oxide (Unuabonah et al. 2007).

Table 3 Thermodynamic parameters for phosphate adsorption onto $Nb_2O_5{\cdot}3H_2O$

T (K)	ΔG° (kJ mol^{-1})	ΔH° (kJ mol^{-1})	ΔS° (J mol^{-1} K^{-1})
298	−17.70	22.30	134.25
308	−19.05		
318	−20.39		
328	−21.73		
338	−23.07		

3.7 Desorption

Repeated availability is an important factor for an advanced adsorbent. Such adsorbent not only possesses higher adsorption capability, but also shows better desorption property, which will significantly reduce overall cost for adsorbent. According to the results of desorption studies, the amount of the desorbed P increased with the increase of pH. When pH value is 5 only extracted 11% phosphate immobilized on the adsorbent. If pH reached 12, 68% could be liberated into the liquid. The results of these desorption studies indicate that the P adsorption on the hydrous niobium is not completely reversible and phosphate can be desorbed from the surface of hydrous niobium oxide by adjusting the pH values of the solution. Effects of pH and desorption studies show that chemisorptions, physisorptions and ion-exchange mechanisms are operative in the adsorption process. Chemisorption involves niobium–phosphate complex formation. Only the phosphate ions that are adsorbed by physisorption and ion exchange are desorbed and the phosphate ions that are removed by complex formation are not desorbed (Namasivayam and Sangeetha 2004).

4 Conclusion

The kinetic process was described by a pseudo-second-order rate model very well. The phosphate adsorption onto $Nb_2O_5{\cdot}3H_2O$ tended to increase with a decrease of pH. The adsorption data fitted well to the Langmuir model with which the maximum P adsorption capacity was estimated to be 18.36 mg-P g^{-1}. The peak appearing at 1050 cm^{-1} in IR spectra after adsorption was attributed to the bending vibration of adsorbed phosphate. The positive values of both ΔH° and ΔS° suggest an endothermic reaction and increase in randomness at the solid-liquid interface during the adsorption. ΔG° values obtained were negative indicating a spontaneous adsorption process. A phosphate desorbability of approximately 68% was observed with water at pH 12, which indicated a relatively strong bonding between the adsorbed phosphate and the sorptive sites on the surface of the adsorbent. The adsorption of phosphate probably occurs by

the mechanisms of ion exchange and physicochemical attraction. Due to its high adsorption capacity, this type of hydrous niobium oxide has the potential for application to control phosphorus pollution.

Acknowledgement L.A.R. would like to acknowledge financial support from Fundação de Amparo à Pesquisa do Estado de São Paulo (FAPESP) grant number 2006/05421-0.

References

Antelo, J., Avena, M., Fiol, S., López, R., Arce, F.: Effects of pH and ionic strength on the adsorption of phosphate and arsenate at the goethite–water interface. J. Colloid Interface Sci. **285**, 476–486 (2005)

Antelo, J., Arce, F., Avena, M., Fiol, S., López, R., Macías, F.: Adsorption of a soil humic acid at the surface of goethite and its competitive interaction with phosphate. Geoderma **138**, 12–19 (2007)

Blaney, L.M., Cinar, S., SenGupta, A.K.: Hybrid anion exchanger for trace phosphate removal from water and wastewater. Water Res. **41**, 1603–1613 (2007)

Borggaard, O.K., Raben-Lange, B., Gimsing, A.L., Strobel, B.W.: Influence of humic substances on phosphate adsorption by aluminium and iron oxides. Geoderma **127**, 270–279 (2005)

Chen, C., Li, X., Zhao, D., Tan, X., Wang, X.: Adsorption kinetic, thermodynamic and desorption studies of Th(IV) on oxidized multiwall carbon nanotubes. Colloids Surf. A **302**, 449–454 (2007)

Chitrakar, R., Tezuka, S., Sonoda, A., Sakane, K., Ooi, K., Hirotsu, T.: Adsorption of phosphate from seawater on calcined MgMn-layered double hydroxides. J. Colloid Interface Sci. **290**, 45–51 (2005)

Chitrakar, R., Tezuka, S., Sonoda, A., Sakane, K., Ooi, K., Hirotsu, T.: Selective adsorption of phosphate from seawater and wastewater by amorphous zirconium hydroxide. J. Colloid Interface Sci. **297**, 426–433 (2006)

Chubar, N.I., Kanibolotskyy, V.A., Strelko, V.V., Gallios, G.G., Samanidou, V.F., Shaposhnikova, T.O., Milgrandt, V.G., Zhuravlev, I.Z.: Adsorption of phosphate ions on novel inorganic ion exchangers. Colloids Surf. A **255**, 55–63 (2005)

Das, J., Patra, B.S., Baliarsingh, N., Parida, K.M.: Adsorption of phosphate by layered double hydroxides in aqueous solutions. Appl. Clay Sci. **32**, 252–260 (2006)

Deliyanni, E.A., Peleka, E.N., Lazaridis, N.K.: Comparative study of phosphates removal from aqueous solutions by nanocrystalline akaganéite and hybrid surfactant-akaganéite. Sep. Purif. Technol. **52**, 478–486 (2007)

Du, X., Yuan, Q., Li, Y.: Equilibrium, thermodynamics and breakthrough studies for adsorption of solanesol onto macroporous resins. Chem. Eng. Process. **47**, 1420–1427 (2008)

Gomri, S., Seguin, J.-L., Guerin, J., Aguir, A.: Adsorption–desorption noise in gas sensors: modelling using Langmuir and Wolkenstein models for adsorption. Sens. Actuators B **114**, 451–459 (2006)

Hameed, B.H., Ahmad, A.A., Aziz, N.: Isotherms, kinetics and thermodynamics of acid dye adsorption on activated palm ash. Chem. Eng. J. **133**, 195–203 (2007)

Harvey, O.R., Rhue, R.D.: Kinetics and energetics of phosphate sorption in a multi-component Al(III)–Fe(III) hydr(oxide) sorbent system. J. Colloid Interface Sci. **322**, 384–393 (2008)

Huang, W., Wang, S., Zhu, Z., Li, L., Yao, X., Rudolph, V., Haghseresht, F.: Phosphate removal from wastewater using red mud. J. Hazard. Mater. **158**, 35–42 (2008)

Inoue, Y., Tochiyama, O., Yamazaki, H., Sakurada, A.: Mechanism of metal-ion sorption on hydrous metal oxides. J. Radioanal. Nucl. Chem. **124**, 361–382 (1988)

Karaca, S., Gürses, A., Ejder, M., Açikyildiz, M.: Kinetic modeling of liquid-phase adsorption of phosphate on dolomite. J. Colloid Interface Sci. **277**, 257–263 (2004)

Karageorgiou, K., Paschalis, M., Anastassakis, G.N.: Removal of phosphate species from solution by adsorption onto calcite used as natural adsorbent. J. Hazard. Mater. **139**, 447–452 (2007)

Krishnan, K.A., Haridas, A.: Removal of phosphate from aqueous solutions and sewage using natural and surface modified coir pith. J. Hazard. Mater. **152**, 527–535 (2008)

Limousin, G., Gaudet, J.-P., Charlet, L., Szenknect, S., Barthès, V., Krimissa, M.: Sorption isotherms: a review on physical bases, modeling and measurement. Appl. Geochem. **22**, 249–275 (2007)

Liu, H., Sun, X., Yin, C., Hu, C.: Removal of phosphate by mesoporous ZrO_2. J. Hazard. Mater. **151**, 616–622 (2008)

Lorenc-Grabowska, E., Gryglewicz, G.: Adsorption of lignite-derived humic acids on coal-based mesoporous activated carbons. J. Colloid Interface Sci. **284**, 416–423 (2005)

Luengo, C., Brigante, M., Antelo, J., Avena, M.: Kinetics of phosphate adsorption on goethite: comparing batch adsorption and ATR-IR measurements. J. Colloid Interface Sci. **300**, 511–518 (2006)

Manna, B., Ghosh, U.C.: Adsorption of arsenic from aqueous solution on synthetic hydrous stannic oxide. J. Hazard. Mater. **144**, 522–531 (2007)

Mulinari, D.R., Rodrigues, L.A., Silva, M.L.C.P.: Adsorção de íons fosfato nos compósitos celulose/ZrO2.nH2O preparados pelos métodos da precipitação convencional e em solução homogênea. Cerâmica **53**, 345–353 (2007)

Namasivayam, C., Sangeetha, D.: Equilibrium and kinetic studies of adsorption of phosphate onto $ZnCl_2$ activated coir pith carbon. J. Colloid Interface Sci. **280**, 359–365 (2004)

Nowack, B., Stone, A.T.: Competitive adsorption of phosphate and phosphonates onto goethite. Water Res. **40**, 2201–2209 (2006)

Oguz, E.: Thermodynamic and kinetic investigations of PO_4^{3-} adsorption on blast furnace slag. J. Colloid Interface Sci. **281**, 62–67 (2005)

Özacar, M.: Contact time optimization of two-stage batch adsorber design using second-order kinetic model for the adsorption of phosphate onto alunite. J. Hazard. Mater. **137**, 218–225 (2006)

Radojevic, M., Bashkin, V.N.: Practical Environmental Analysis. MPG Books, Cornwal (1999)

Ren, Y., Wei, X., Zhang, M.: Adsorption character for removal Cu(II) by magnetic Cu(II) ion imprinted composite adsorbent. J. Hazard. Mater. **158**, 14–22 (2008)

Rodgher, S., Espíndola, E.L.G., Rocha, O., Fracácio, R., Pereira, R.H.G., Rodrigues, M.H.S.: Limnological and ecotoxicological studies in the cascade of reservoirs in the Tietê river (São Paulo, Brazil). Braz. J. Biol. **65**, 697–710 (2005)

Rodrigues, L.A., Silva, M.L.C.P.: Estudo da adsorção de íons fosfato em matriz inorgânica. Cerâmica **54**, 92–96 (2008)

Sodré, F.F., Lenzi, E., Costa, A.C.S.: Utilização de modelos físico-químicos de adsorção no estudo do comportamento do cobre em solos argilosos. Quim. Nova **24**, 324–330 (2001)

Spinelli, V.A., Laranjeira, M.C.M., Favere, V.T.: Cinética e equilíbrio de adsorção dos oxiânions Cr(VI), Mo(VI) e Se(VI) pelo sal de amônio quaternário de quitosana. Polímeros **15**, 218–223 (2005)

Tagliaferro, G.V., Silva, G.L.J.P., Silva, M.L.C.P.: Influência do agente precipitante na preparação do óxido de nióbio (v) hidratado pelo método da precipitação em solução homogênea. Quim. Nova **28**, 250–254 (2005)

Unuabonah, E.I., Adebowale, K.O., Olu-Owolabi, B.I.: Kinetic and thermodynamic studies of the adsorption of lead (II) ions onto phosphate-modified kaolinite clay. J. Hazard. Mater. **144**, 386–395 (2007)

Wang, S.-L., Cheng, C.-Y., Tzou, Y.-M., Liaw, R.-B., Chang, T.-W., Chen, J.-H.: Phosphate removal from water using lithium intercalated gibbsite. J. Hazard. Mater. **147**, 205–212 (2007)

Xiaofang, Y., Dongsheng, W., Zhongxi, S., Hongxiao, T.: Adsorption of phosphate at the aluminum (hydr)oxides–water interface: role of the surface acid–base properties. Colloids Surf. A **297**, 84–90 (2007)

Xiong, J., He, Z., Mahmood, Q., Liu, D., Yang, X., Islam, E.: Phosphate removal from solution using steel slag through magnetic separation. J. Hazard. Mater. **152**, 211–215 (2008)

Ye, H., Chen, F., Sheng, Y., Sheng, G., Fu, G.: Adsorption of phosphate from aqueous solution onto modified palygorskites. Sep. Purif. Technol. **50**, 283–290 (2006)

Zhong, B., Stanforth, R., Wu, S., Chen, J.P.: Proton interaction in phosphate adsorption onto goethite. J. Colloid Interface Sci. **308**, 40–48 (2007)